

Formation of starch-guest inclusion complexes in electrospun  
starch fibers

Lingyan Kong – Pennsylvania State  
University

Gregory R. Ziegler – Pennsylvania State  
University

Deposited 04/29/2020

Citation of published version:

Kong, L., Ziegler, G. (2014): Formation of starch-guest inclusion complexes in electrospun starch fibers. *Food Hydrocolloids*, vol. 38.

DOI: <https://doi.org/10.1016/j.foodhyd.2013.12.018>



This work is licensed under a [Creative Commons Attribution-NonCommercial-NoDerivatives 4.0 International License](https://creativecommons.org/licenses/by-nc-nd/4.0/).

Full text at <https://doi.org/10.1016/j.foodhyd.2013.12.018>

or send request to [lingyan.kong@ua.edu](mailto:lingyan.kong@ua.edu)

1

2     **Formation of starch-guest inclusion complexes in electrospun**

3                                     **starch fibers**

4

5                                     *Lingyan Kong, and Gregory R. Ziegler\**

6                                     Department of Food Science

7                                     Pennsylvania State University

8                                     341 Food Science Building

9                                     University Park, PA 16802

10

11    For submission to: *Food Hydrocolloids*

12    E-Mail: [grz1@psu.edu](mailto:grz1@psu.edu)

13    \* Author to whom correspondence should be addressed; Tel.: +1-814-863-2960; Fax: +1-814-  
14    863-6132; E-Mail: [grz1@psu.edu](mailto:grz1@psu.edu)

15

16 ABSTRACT: We have demonstrated a method of fabricating starch fibers with an average  
17 diameter in the order of micrometers. In the present study, the formation of starch-guest  
18 inclusion complexes in the electrospun starch fibers was evaluated. Two methods were used to  
19 electrospin starch fibers with starch-guest inclusion complexes: a dope mixing method, where guest  
20 material was mixed into the starch dispersion prior to electrospinning, and a bath mixing method,  
21 where guest material was mixed into the coagulation bath into which starch dispersions were  
22 electrospun. Three selected guest compounds, palmitic acid, ascorbyl palmitate, and cetyl-  
23 trimethylammonium bromide, formed inclusion complexes with starch in the electrospun starch  
24 fibers. The presence of native lipids was not necessary to induce the inclusion complex formation.  
25 Encapsulation of these molecules in electrospun starch fibers may increase their stability during  
26 processing and storage, while providing controlled release properties.

27 KEYWORDS: starch, inclusion complex, molecular encapsulation, electrospinning, fiber.

## 28 **1. Introduction**

29 Starch, especially its amylose component, is well known to form inclusion complexes with a  
30 variety of small molecules, e.g. iodine (Bluhm & Zugenmaier, 1981), alcohols (Whittam et al.,  
31 1989), fatty acids (Biliaderis, Page, Slade, & Sirett, 1985), aromas (Pozo-Bayon, Biais, Rampon,  
32 Cayot, & Le Bail, 2008), salicylic acid (Oguchi, Yamasato, Limmatvapirat, Yonemochi, &  
33 Yamamoto, 1998) and its analogues (Uchino, Tozuka, Oguchi, & Yamamoto, 2002), and  
34 ibuprofen (Yang et al., 2013). In the presence of many guest molecules, amylose forms a 6-fold  
35 left-handed single helix stabilized by hydrogen bonds (Conde-Petit, Escher, & Nuessli, 2006).  
36 The amylose helices may then pack together forming a crystalline structure known as the V-type.  
37 The amylose helix has a hydrophilic outer surface and a hydrophobic helical channel that  
38 accommodates the guest molecules (intrahelical association). Crystals of such intra-helical  
39 inclusion complexes are known as sub-type  $V_{6I}$  (aka V-hydrate or  $V_h$ ), or anhydrous V ( $V_a$ ) on  
40 losing water from between the helices (Winter & Sarko, 1974). Alternatively, guest molecules  
41 can also be entrapped between amylose helices (interhelical association) in sub-type  $V_{6II}$  (or  
42  $V_{butanol}$ ) and  $V_{6III}$  (or  $V_{isopropanol}$ ), which have larger inter-helical space than  $V_{6I}$  (Helbert &  
43 Chanzy, 1994; Rondeau-Mouro, Bail, & Buléon, 2004). In the absence of inclusion complex  
44 formation, materials may be simply entrapped in the starch matrix in a process known as  
45 microencapsulation (Shimoni, 2008).

46 Amylose-guest inclusion complexes may be useful as a delivery system for guest molecules.  
47 For instance, amylose complexed with conjugated linoleic acid (Lalush, Bar, Zakaria, Eichler, &  
48 Shimoni, 2004), genistein (Cohen, Orlova, Kovalev, Ungar, & Shimoni, 2008), esters of vitamin  
49 and fatty acid (Lay Ma, Floros, & Ziegler, 2011), and long chain unsaturated fatty acids (Lesmes,  
50 Barchechath, & Shimoni, 2008; Lesmes, Cohen, Shener, & Shimoni, 2009) have been produced  
51 for controlled release purposes. By forming an inclusion complex with amylose or starch, it is

52 expected that the active ingredients, such as essential fatty acids, lipophilic vitamins, and soy  
53 isoflavones, can be protected against the acidic environment of the stomach, and their  
54 bioavailability may be increased, since the bioactive guest compounds can be released in the  
55 small intestine by the action of enzymes (Yang, Gu, & Zhang, 2009).

56 There are mainly three methods to prepare amylose-guest inclusion complexes: the high  
57 temperature method, the dimethyl sulfoxide (DMSO) method and the alkali method (Putseys,  
58 Lamberts, & Delcour, 2010). The general idea is to first obtain random coils or loose helices of  
59 amylose molecules by dissolution in water (e.g. at 160 °C), in DMSO (e.g. 95% (v/v) DMSO) or  
60 in alkali (e.g. 0.01 M potassium hydroxide) solutions, respectively. After which the desired guest  
61 can be mixed into the amylose dispersion. In the high temperature method, the mixture is  
62 allowed to cool down slowly and the inclusion complexes formed will crystallize. In the DMSO  
63 method, the solution is diluted with water at an elevated temperature and allowed to cool slowly.  
64 The inclusion complexes formed will then crystallize and precipitate. In the alkali method, the  
65 solution is neutralized and slowly cooled prior to precipitation.

66 We have recently fabricated starch fibers by an electrospinning method and studied the  
67 effect of solution rheological properties and spinning parameters on fiber formation (Kong &  
68 Ziegler, 2012a, 2012b, 2013, 2014). These electrospun starch fibers showed V-type X-ray  
69 diffraction patterns, especially when using a coagulation bath with ethanol concentrations above  
70 50% (v/v) suggesting this may be a new method to prepare starch-guest complexes (Kong &  
71 Ziegler, 2014).

72 A nonwoven starch fiber mat may find use in biomedical applications, especially wound  
73 dressings and drug delivery. Fibers have a greater surface area compared with current wound  
74 dressings and delivery matrices based on foams, films and hydrogels. The high effective surface  
75 area promotes hemostasis, extrudate absorption, and cell proliferation (Zahedi, Rezaeian, Ranaei-

76 Siadat, Jafari, & Supaphol, 2010). The porous 3-dimensional structure and small pore size enable  
77 the respiration of cells as well as protect the wound from bacterial infection, and compared with  
78 traditional petroleum-based synthetic dressing materials, such as nylon and polystyrene, starch is  
79 lower in cost and biodegradable, with a sustainable supply. Starch fibers can be absorbed by the  
80 human body without any allergic or toxic side effects. Hence the opportunity to develop active  
81 wound dressings and drug delivery systems if drugs, nutrients or bioactive compounds can be  
82 complexed inter-helically or intra-helically within the starch fibers.

83 The objectives of the present study were to investigate the formation of inclusion complexes  
84 of high amylose starch with palmitic acid (PA), ascorbyl palmitate (AP), and cetyl-  
85 trimethylammonium bromide (CTAB) in electrospun starch fibers. AP is an ester form of  
86 ascorbic acid (vitamin C) with palmitic acid and has been used as a source of vitamin C and an  
87 antioxidant food additive. CTAB can be used as a cationic surfactant and an effective antiseptic  
88 agent against bacteria and fungi. All of these three guest compounds have 16-carbon alkyl chains  
89 and have been shown to readily form complexes with starch using conventional methods  
90 (Bhosale & Ziegler, 2010; Eliasson, 1988; Lay Ma et al., 2011). Two inclusion forming methods  
91 during electrospinning were evaluated, namely a dope mixing method and a bath mixing method.  
92 For each compound, the effects of guest concentration and ethanol concentration in the  
93 coagulation bath were also studied. Complementary techniques were employed to determine  
94 whether the guest molecules were molecularly included into the starch helices.

## 95 **2. Materials and Methods**

### 96 **2.1. Materials**

97 High amylose maize starch (Hylon VII) was kindly provided by Ingredion Incorporated  
98 (Bridgewater, NJ). Dimethyl sulfoxide (DMSO) and Ethanol (200 proof) were obtained from

99 VWR International (Radnor, PA). Guest material cetyl trimethylammonium bromide (CTAB)  
100 was obtained from J. T. Baker (Philipsburg, NJ), palmitic acid (PA) from Eastman Kodak  
101 Company (Rochester, NY), and ascorbyl palmitate (AP) from Sigma–Aldrich, Inc (St. Louis,  
102 MO). Lipid-free Hylon VII starch was produced by dispersing the starch in 90% DMSO aqueous  
103 solution followed by ethanol precipitation (Klucinec & Thompson, 1998). Electrospinning of  
104 lipid-free starch with and without AP was conducted as a control experiment to exclude native  
105 lipids as the sole guest in inclusion complex formation.

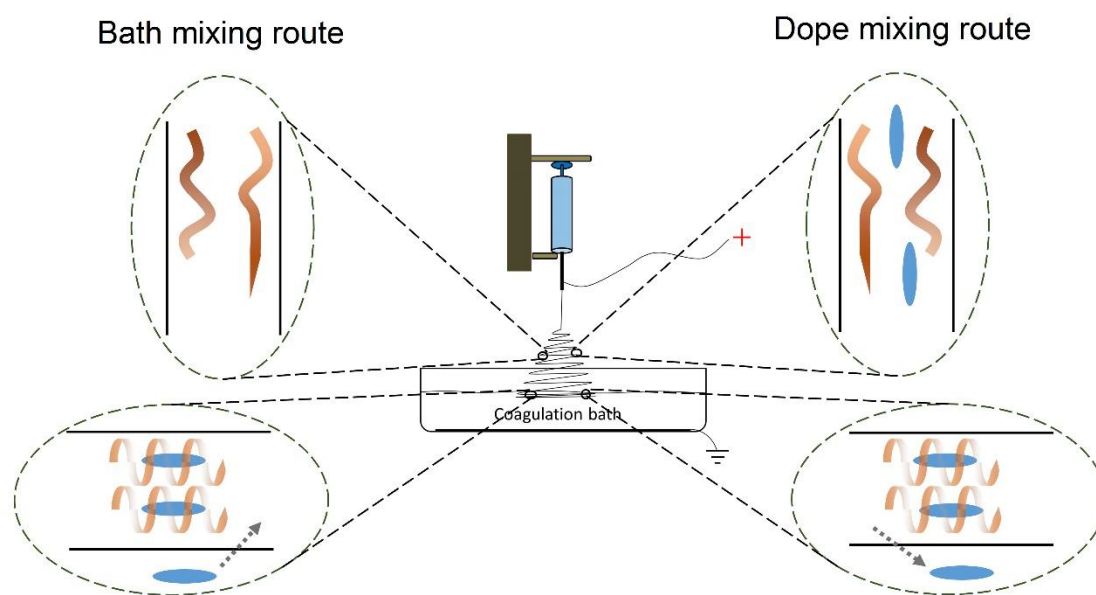
## 106 **2.2. Electrospinning**

107 The electrospinning setup (Fig. 1) used in this study contained a high voltage generator  
108 (ES40P, Gamma High Voltage Research, Inc., Ormond Beach, FL), a syringe pump (81620,  
109 Hamilton Company, Reno, NV), and a grounded metal mesh immersed in an ethanol/water  
110 mixture. A 10 ml syringe (Becton, Dickinson and Company, Franklin Lakes, NJ) with a 20  
111 gauge blunt needle was used to extrude the starch dispersion for electrospinning (Kong &  
112 Ziegler, 2012b). This electrospinning configuration can also be referred to as “electro-wet-  
113 spinning”. Electrospinning was conducted at room temperature in this study. Feed rate was set at  
114 4 ml/h, spinning distance at 7.5 cm and voltage at 7.5 kV. The fibrous mat deposited in the  
115 coagulation bath was kept for 5 min and then washed using ethanol (~50 mL for first wash and  
116 ~10 mL for second wash) and dried in a desiccator containing Drierite under vacuum.

## 117 **2.3. Inclusion complex formation during electrospinning**

118 Two different means of including guest material were evaluated in this study (Fig. 1). **Dope**  
119 **mixing method:** in this method, the guest material was mixed with the starch dispersion prior to  
120 electrospinning. In detail, 15% (w/v) of starch was dissolved in a 95% (v/v) DMSO aqueous  
121 solution. The starch dispersion was heated in a boiling water bath with continuous stirring on a

122 magnetic stirrer hotplate for about one hour. Heat-stable guests (e.g. PA) were mixed into the  
123 starch dispersion during heating, while heat-labile guests (e.g. AP) were mixed after the  
124 homogenous dispersion was cooled to room temperature. **Bath mixing method:** the guest  
125 compounds were mixed into the coagulation bath (100 ml) to achieve a concentration from 0.1%  
126 to 0.5% (w/v) for AP and from 0.1% to 2% (w/v) for CTAB. About 1-2 ml of 15% (w/v) starch  
127 dispersion was then electrospun into the coagulation bath. In both methods, two coagulation bath  
128 compositions, 100% (v/v) and 75% (v/v) aqueous ethanol solutions, were evaluated in terms of  
129 inclusion complex formation.



130  
131 **Fig. 1.** Schematic drawing of the electro-wet-spinning setup and two routes of starch-guest  
132 inclusion complex formation during electrospinning. Orange curves show the conformation of  
133 starch molecules and blue ovals stand for guest molecules. Grey arrows show the diffusion of  
134 guest molecules either into or out of the precipitated fibers.

#### 135 **2.4. Inclusion complex formation by DMSO method**

136 Starch (500 mg) was dissolved in 10 mL of 95% (v/v) DMSO aqueous solution in a boiling  
137 water bath with constant stirring for at least one hour. Then 1 mL of guest (50 mg) solution in  
138 95% DMSO preheated at 90 °C were mixed with the starch solution at 90 °C. The mixed solution  
139 was held for 15 minutes at 90 °C, after which 25 mL of distilled water preheated at 90 °C was  
140 rapidly added to the solution with vigorous stirring. The sample solution was incubated for 15  
141 min at 90 °C, the heater turned off, and samples were allowed to cool for at least 24 hours.  
142 Inclusion complexes were recovered by centrifugation, washed three times with 50% (v/v)  
143 ethanol/water solution, and then washed with 100% ethanol. The resulting pellet was transferred  
144 to an aluminum dish with a small amount of 100% ethanol, and allowed to dry at room  
145 temperature in a desiccator. Dried samples were pulverized into fine powders for further  
146 analysis.

#### 147 **2.5. Wide angle X-ray diffraction (XRD)**

148 XRD patterns were obtained with a Rigaku MiniFlex II desktop X-ray diffractometer  
149 (Rigaku Americas Corporation, TX). Samples were exposed to Cu K $\alpha$  radiation (0.154 nm) and  
150 continuously scanned between  $2\theta = 4$  and  $30^\circ$  at a scanning rate of  $1^\circ/\text{min}$  with a step size of  
151  $0.02^\circ$ . A current of 15 mA and voltage of 30 kV were used. Data were analyzed with Jade v.8  
152 software (Material Data Inc., Livermore, CA). The area of the amorphous halo generated by Jade  
153 software using the cubic spline fit option was subtracted from the total X-ray diffraction area to  
154 obtain the crystalline fraction. The degree of crystallinity was then calculated as the crystalline  
155 fraction over the total area multiplied by 100.

## 156 **2.6. Differential scanning calorimetry (DSC)**

157        Approximately 5 mg of sample was weighed into a 60  $\mu$ L stainless steel DSC pan (Perkin-  
158 Elmer Instruments, Norwalk, CT) and water added to obtain a 10% (w/v) dispersion. Pans were  
159 hermetically sealed. Samples were equilibrated to 20  $^{\circ}$ C, and then heated to 170  $^{\circ}$ C at 2  $^{\circ}$ C /min  
160 in a Thermal Advantage Q100 DSC (TA Instruments, New Castle, DE). The DSC was calibrated  
161 with indium, with an empty sample pan used as the reference. Data was analyzed using the TA  
162 Universal Analysis software (Universal Analysis 2000 v.4.2E, TA Instruments-Waters LLC,  
163 New Castle, DE).

## 164 **2.7. Fourier transformed infrared (FTIR) spectroscopy**

165        FTIR analysis of electrospun starch fibers was performed on a Bruker IFS 66/S FT-IR  
166 Spectrometer (Bruker Optics Ltd., Billerica, MA) equipped with a Hyperion 3000 FT-IR  
167 Microscope. Spectra of thin sections of fiber mat were obtained by an accumulation of 400 scans  
168 in transmission mode from 500  $\text{cm}^{-1}$  to 4000  $\text{cm}^{-1}$  with a resolution of 6  $\text{cm}^{-1}$ . For powder  
169 samples, FTIR was performed on a Bruker v70 Spectrometer (Bruker Optics Inc., Billerica, MA)  
170 equipped with an MVP-Pro<sup>TM</sup> Star Diamond attenuated total reflectance (ATR) accessory  
171 (Harrick Scientific Products, Inc., Pleasantville, NY). The spectra were scanned at room  
172 temperature over the wave number range of 400 to 4000  $\text{cm}^{-1}$ , with an accumulation of 100  
173 scans and a resolution of 6  $\text{cm}^{-1}$ .

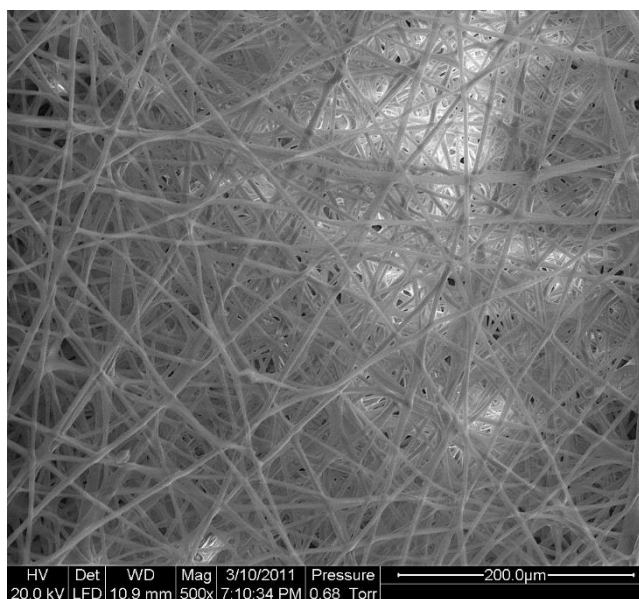
## 174 **2.8. Scanning electron microscopy (SEM)**

175        Observation of fibers was performed using a FEI Quanta 200 environmental scanning  
176 electron microscope (ESEM, FEI, Hillsboro, OR) in low vacuum mode at an accelerating voltage  
177 of 20 keV. Fiber diameter was measured from the ESEM images.

178 **3. Results and Discussion**

179 **3.1. Inclusion complex formation in electrospun fibers: dope mixing method**

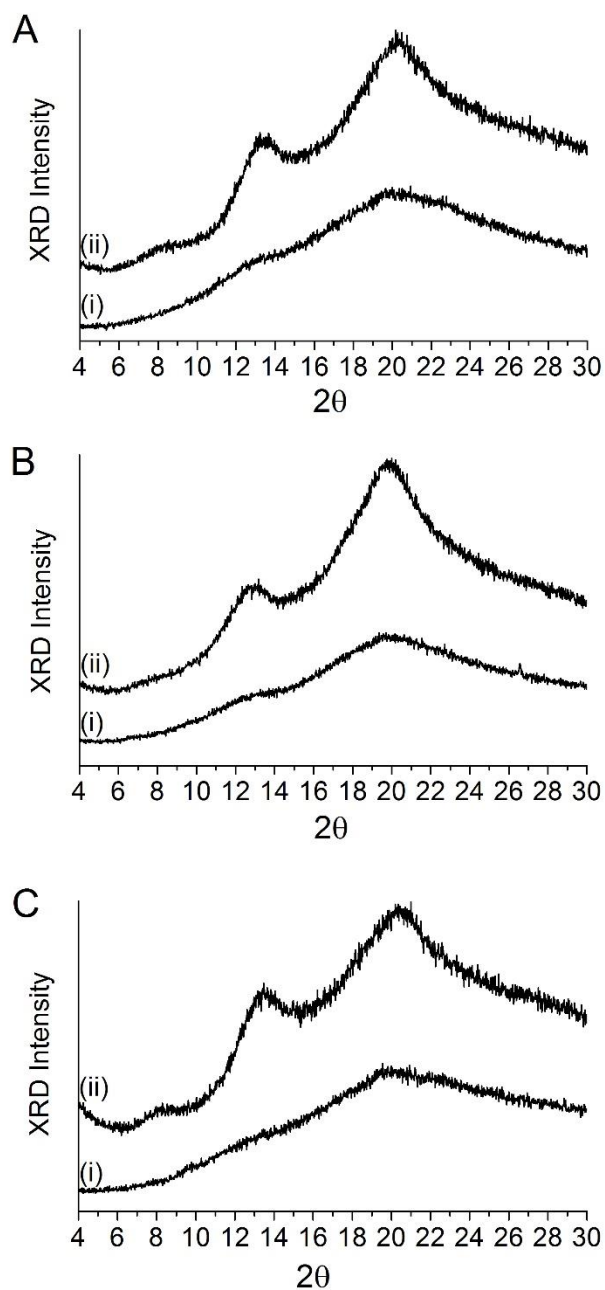
180 Three different guest compounds were mixed into the starch dispersion before  
181 electrospinning. During initial trials the addition of guest compounds affected the  
182 electrospinnability of the starch dispersions. A 15% (w/v) starch dispersion with more than 5%  
183 palmitic acid (PA) was not electrospinnable because of an increase in viscosity, while the  
184 addition of CTAB made the jet unstable probably due to change in conductivity and surface  
185 tension of the dispersion. Hence, PA and ascorbyl palmitate (AP) were added up to 5% of starch  
186 weight for electrospinning. Fiber morphology (Fig. 2) was similar to that previously reported for  
187 starch without guest compounds (Kong & Ziegler, 2014).



188  
189 **Fig. 2.** Scanning electron micrograph of starch-palmitic acid fibers from coagulation bath  
190 containing 75% (v/v) ethanol.

191 The X-ray diffraction patterns of starch-PA and starch-AP fibers deposited into either 100%  
192 or 75% (v/v) ethanol were similar to those without guest compounds added (Fig. 3). The level of  
193 guest addition did not affect the peak intensities or positions in XRD patterns, so XRD patterns

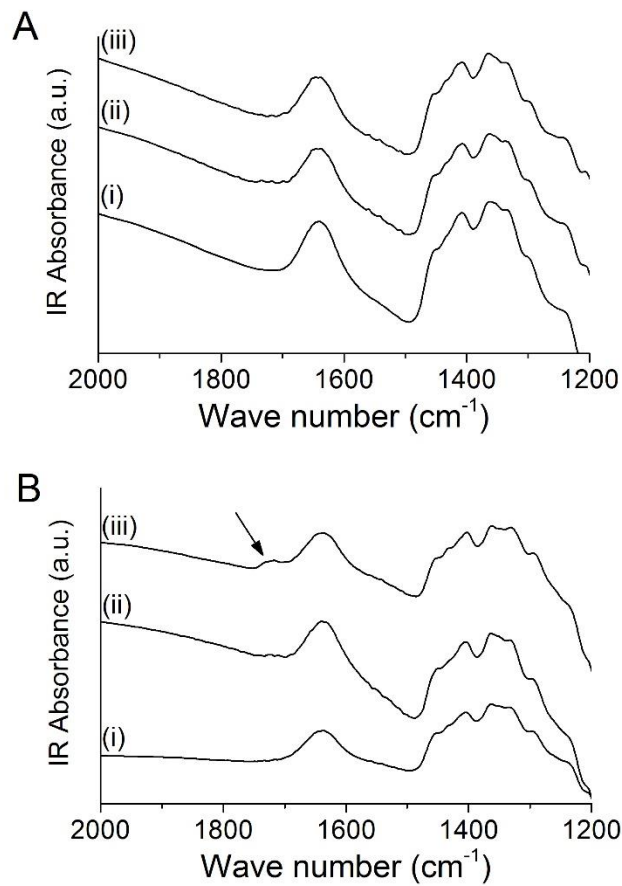
194 as a function of guest concentration are not shown. The fibers from 75% ethanol coagulation  
195 bath all displayed V-type X-ray diffraction patterns. The  $V_{6I}$ -type patterns suggested that guest  
196 compounds, if included, were entrapped intra-helically instead of inter-helically (Rondeau-  
197 Mouro et al., 2004). The crystallinity was estimated to be 30% and 26% for starch-PA and  
198 starch-AP fibers, respectively. The fibers from 100% ethanol coagulation bath showed a very  
199 weak V-pattern, indicating a lesser extent of inclusion complex formation or the so-called “type I  
200 non-crystalline” inclusion complexes (Biliaderis & Galloway, 1989). Either guest compounds  
201 were not included in starch helices, or starch-guest inclusion complexes were loosely assembled  
202 and arranged in a less regular manner due to rapid starch precipitation in absolute ethanol.  
203 Therefore, additional characterization techniques were needed to determine which explanation  
204 contributed to the inefficiency in inclusion complex formation.



205  
 206 **Fig. 3.** X-ray diffraction patterns of (A) starch without guest, (B) starch-palmitic acid (1%, w/w),  
 207 and (C) starch-ascorbyl palmitate (1%, w/w) fibers from coagulation baths containing (i) 100%  
 208 and (ii) 75% (v/v) ethanol, respectively.

209 FTIR has been employed to quantify the amount of included guest compounds in starch  
 210 (Biais, Le Bail, Robert, Pontoire, & Buléon, 2006; Uchino et al., 2002). Here, FTIR was used to  
 211 determine the presence of guest compounds in the starch fibers (Fig. 4 & 5). The carbonyl

212 stretching band ranging from approximately 1690 to 1760  $\text{cm}^{-1}$  is the only distinguishable band  
213 for PA and AP in a starch matrix. Therefore, we limited our analysis to IR spectra in a narrow  
214 wavenumber range. Starch-PA and starch-AP fibers spun into 100% ethanol did not show any  
215 characteristic peaks for PA or AP. At 5% of PA, starch-PA fibers spun into 75% ethanol  
216 displayed a peak at around 1722  $\text{cm}^{-1}$ , which is attributed to the carbonyl group in PA. The  
217 carbonyl bands in raw PA and AP powders were positioned at about 1696 and 1730  $\text{cm}^{-1}$ ,  
218 respectively (Spectra of PA and AP can be found in supplementary material, Fig. A.). This  
219 characteristic peak for the carbonyl group was found in starch-AP fibers with 1% of AP mixed  
220 into the spinning dope. However, the peaks shifted slightly to a higher wave number at 1735  $\text{cm}^{-1}$   
221 in 5% AP added starch fibers. A shift of the carbonyl peak in FTIR spectra has been reported for  
222 the amylose-AP inclusion complex (Lay Ma et al., 2011) and amylose complexes with salicylic  
223 acid analogues (Uchino et al., 2002) and *p*-aminobenzoic acid (Tozuka et al., 2006). The shift of  
224 carbonyl peak could be attributed to the breakage of hydrogen bonds between PA/AP molecules  
225 in the crystalline state and the formation of new hydrogen bonds between the carbonyl group of  
226 PA/AP and the hydroxyl group of amylose (Lay Ma et al., 2011). The FTIR results suggested  
227 that by using 100% ethanol as the coagulation bath, few compounds were included into the  
228 starch helices and those uncomplexed helices were loosely and irregularly packed. A coagulation  
229 bath containing 75% ethanol facilitated the inclusion complex formation and improved the  
230 regularity of helical arrangement.

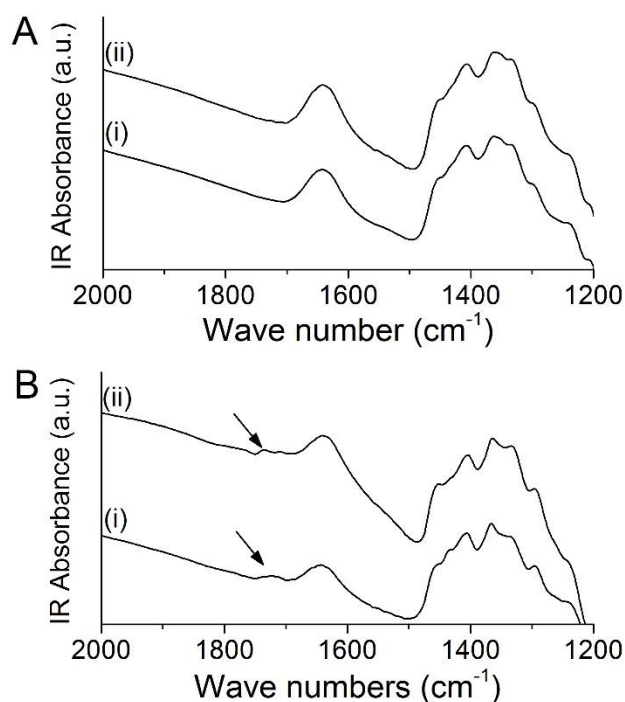


231

232 **Fig. 4.** FTIR spectra of starch-palmitic acid (PA) fibers from coagulation baths containing (A)

233 100% (v/v) and (B) 75% (v/v) ethanol, with different PA levels in spinning dope: (i) 1%, (ii)

234 2.5%, and (iii) 5% (w/w) of starch. Arrows indicate the band for PA.



235  
 236 **Fig. 5.** FTIR spectra of starch-ascorbyl palmitate (AP) fibers from coagulation baths containing  
 237 (A) 100% (v/v) and (B) 75% (v/v) ethanol, with different AP levels in spinning dope: (i) 1%, and  
 238 (ii) 5% (w/w) of starch. Arrows indicate the band for AP.

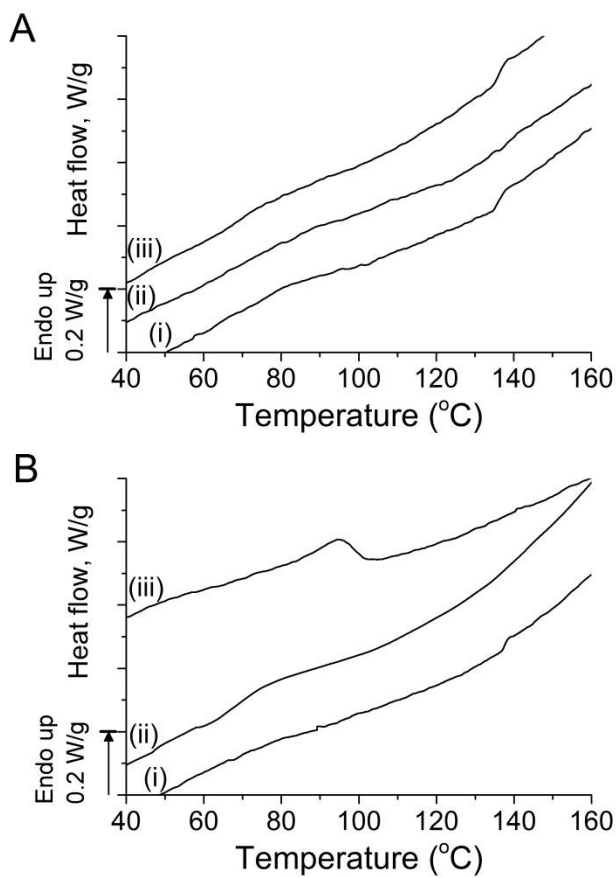
239 Thermograms of starch-PA and starch-AP fibers from 100% ethanol showed a broad and  
 240 flat endotherm between 60 and 100 °C (Fig. 6 & 7), indicating limited complexation. This agrees  
 241 with the weak V-pattern for the fibers from 100% ethanol; a very small amount of PA, AP and  
 242 native lipids in starch could have been included in starch molecules in the fibers. Approximately  
 243 1% (w/w) monoacyl lipids, e.g. palmitic, stearic, and linoleic acid, exist in native high amylose  
 244 maize starch (Morrison, 1988). These lipids are potentially able to form inclusion complexes  
 245 with starch. The presence of these various lipids may have resulted in different structures of  
 246 inclusion complexes, e.g. length of helices, and thus different thermal stabilities of the inclusion  
 247 complexes (Tufvesson, Wahlgren, & Eliasson, 2003). The broad and low endotherms seen might  
 248 also be attributed to the retrogradation of the amylopectin fraction of starch (Kohyama &  
 249 Nishinari, 1991). The thermograms also show an endotherm with a peak temperature about 140

250 °C, which can be attributed to the dissociation of retrograded amylose (Raphaelides & Karkalas,  
251 1988).

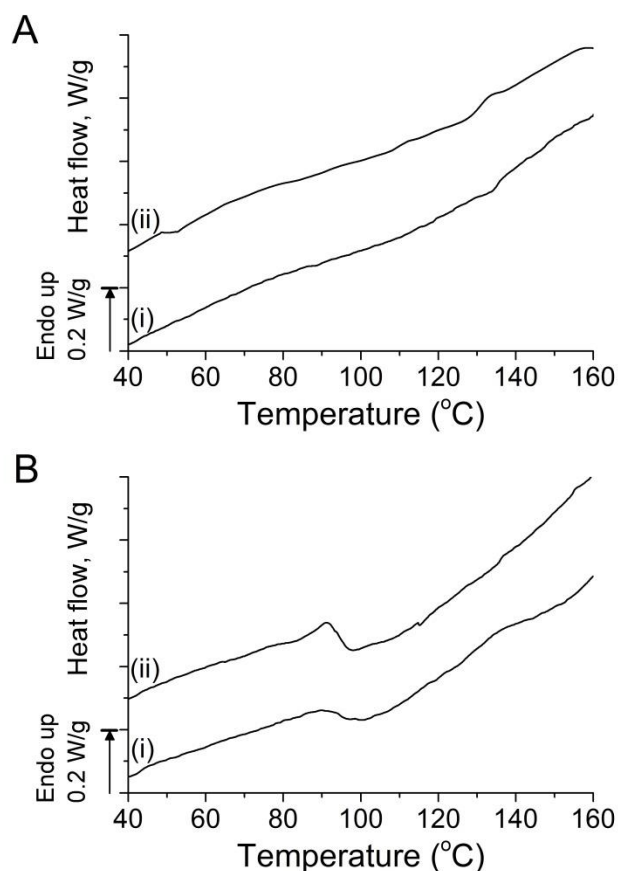
252 A broad and flat endotherm from 50 to 90 °C was observed during heating of starch-PA  
253 fibers from 75% ethanol at a PA level of 1%. The endotherm shifted to higher temperatures (65  
254 to 100 °C), as PA level increased to 2.5%. The broad and flat endotherm was again caused by  
255 different inclusion complex structures with native lipids and PA that was added at low levels.  
256 When 5% PA was added, a single narrow endotherm at around 94.5 °C was observed, which can  
257 be attributed to the dissociation of inclusion complexes mainly between starch and PA. The  
258 enthalpy of dissociation was estimated to be 2.6 J/g. In starch-AP fibers from 75% ethanol, a  
259 single narrow endotherm at around 91 °C was obtained at both AP levels. Higher AP level  
260 resulted in a higher dissociation enthalpy, 3.3 J/g at 5% AP versus 2.0 J/g at 1% AP. The lower  
261 enthalpy at 1% AP indicates a larger portion of uncomplexed starch, which otherwise  
262 retrograded as can be evidenced by an endotherm from 130 to 145 °C. Similar to previous reports  
263 for amylose inclusion complexes (Lay Ma et al., 2011), starch-AP inclusion complexes formed  
264 in the fibers had a lower thermal stability compared with that of starch-PA. This was caused by  
265 the structural difference between the two molecules. The ascorbyl group on AP had steric effect  
266 on inclusion complex formation because it could be difficult for the bulky and hydrophilic  
267 ascorbyl group to enter the internal helix. Hence, there is a possibility that the lower dissociation  
268 temperature was caused by that AP formed shorter helices with starch than PA.

269 Compared with the inclusion complexes formed by the traditional DMSO method, the peak  
270 temperature was the same, but the enthalpy of dissociation was much lower in the fiber samples.  
271 The Hylon VII starch-PA and starch-AP inclusion complexes made by DMSO method had  
272 endothermic peak temperatures at 94.5 °C and 93.2 °C, and enthalpies of 14.3 J/g and 9.8 J/g,  
273 respectively (supplementary material, Fig. B.), which suggests that while same length of helices

274 was formed in both cases, inclusion complex formation during electrospinning of fibers was less  
275 efficient since much less amount of guest was complexed.



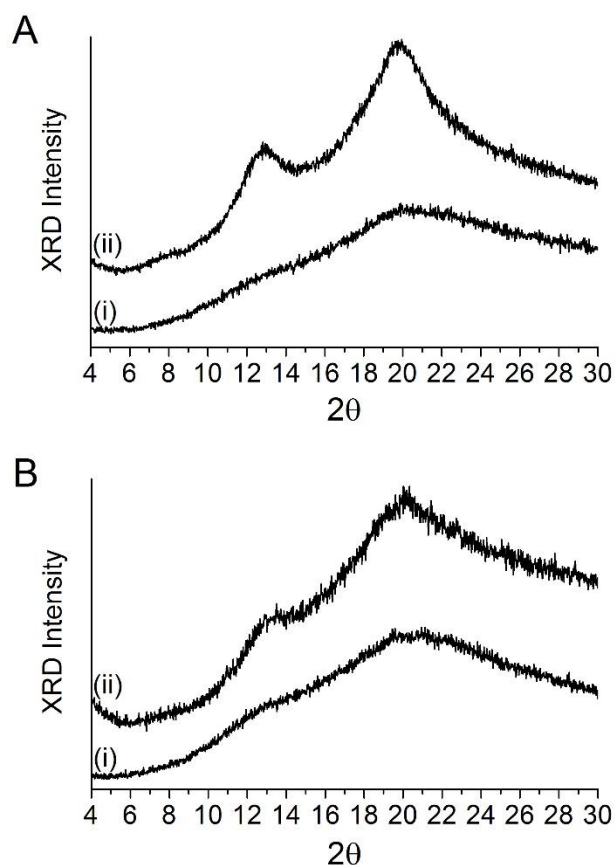
276  
277 **Fig. 6.** DSC curves of starch-palmitic acid (PA) fibers from coagulation baths containing (A)  
278 100% (v/v) and (B) 75% (v/v) ethanol, with different PA levels in spinning dope: (i) 1%, (ii)  
279 2.5%, and (iii) 5% (w/w) of starch.



280  
 281 **Fig. 7.** DSC curves of starch-ascorbyl palmitate (AP) fibers from coagulation baths containing  
 282 (A) 100% (v/v) and (B) 75% (v/v) ethanol, with different AP levels in spinning dope: (i) 1%, and  
 283 (ii) 5% (w/w) of starch.

### 284 3.2. Inclusion complex formation in electrospun fibers: bath mixing method

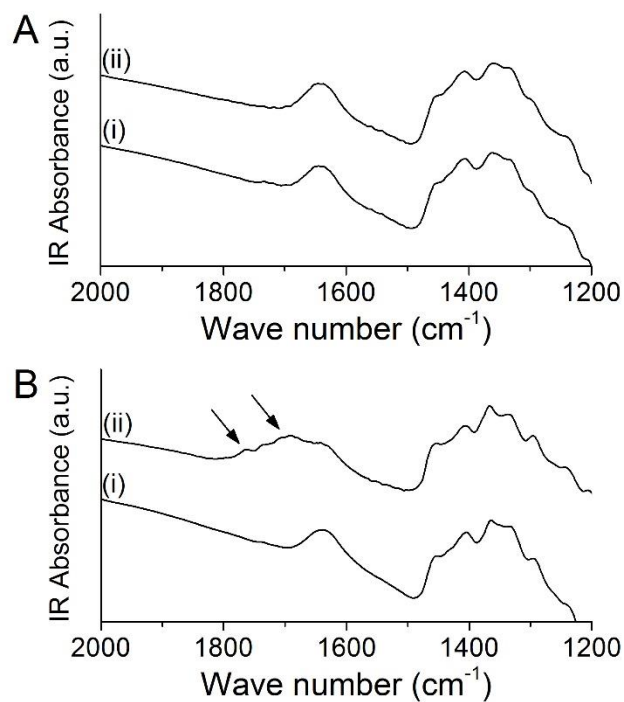
285 AP and CTAB were mixed into the coagulation baths prior to electrospinning of starch  
 286 dispersions, whereas PA was not used due to its low solubility in aqueous ethanol solutions. It  
 287 was hypothesized that as starch precipitated due to the change of solvent environment, guest  
 288 compounds could enter the starch helices. The X-ray patterns of the starch fibers were identical  
 289 to those from coagulation baths without addition of guest compounds (Fig. 8). The V-type X-ray  
 290 diffraction patterns suggested the formation of V-type starch in the fibers, though whether AP  
 291 and CTAB were included could not be ascertained without further FTIR and DSC evidence.



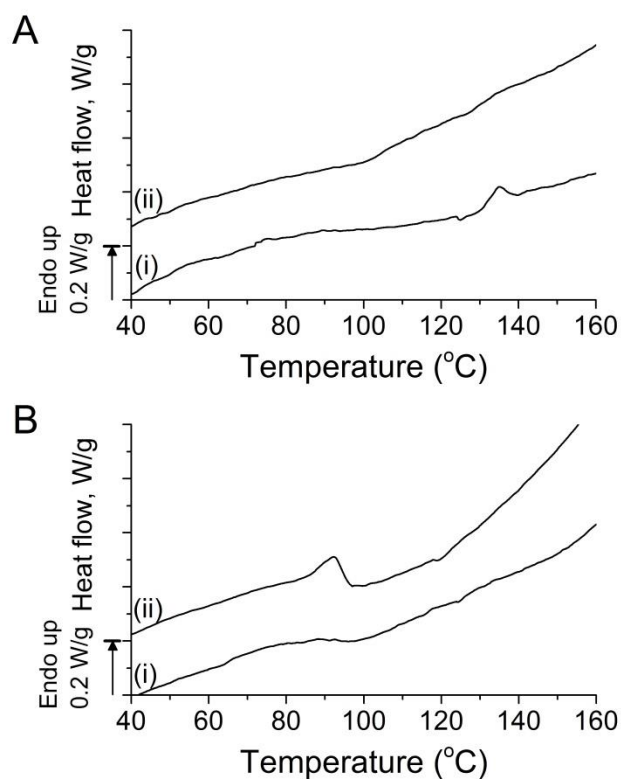
292  
 293 **Fig. 8.** X-ray diffraction patterns of starch fibers from coagulation baths containing (A) 0.5%  
 294 (w/v) AP and (B) 2% (w/v) CTAB in (i) 100% and (ii) 75% (v/v) ethanol, respectively.

295 AP was found to be present in the starch fibers from 75% ethanol according to the FTIR  
 296 spectra (Fig. 9). A characteristic carbonyl band was positioned at about 1733 to 1740  $\text{cm}^{-1}$  for  
 297 starch-AP fibers from both 100% and 75% ethanol with 0.1% AP, indicating a small amount of  
 298 native fatty acids or guest AP, were complexed into starch helices. The heterogeneity of the  
 299 inclusion complex structure was evidenced from the broad and flat endotherm between 50 and  
 300 100  $^{\circ}\text{C}$  for these fiber samples (Fig. 10). When 0.5% AP was mixed into 75% ethanol, the  
 301 carbonyl band of the starch-AP fiber shifted further to an even higher wave number (1764  $\text{cm}^{-1}$ )  
 302 than that by dope mixing method. This shift could be induced by more starch-AP inclusion  
 303 complex formation, which is also evidenced by a higher dissociation enthalpy about 5.8 J/g from  
 304 the thermogram (Fig. 10). The peak endotherm temperature (91  $^{\circ}\text{C}$ ) was the same as that of

305 starch-AP dissociation by the dope mixing method. The difference in guest addition methods did  
306 not affect the helical length of inclusion complexes.



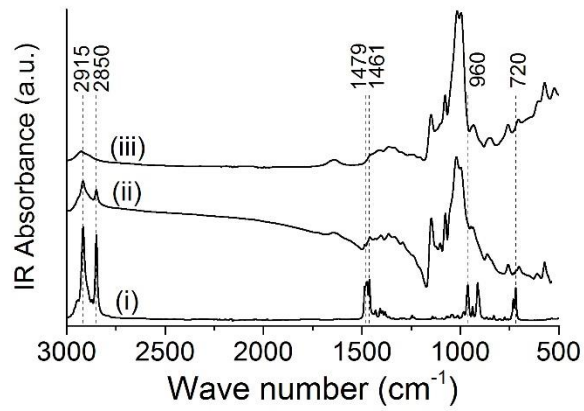
307  
308 **Fig. 9.** FTIR spectra of starch fibers from coagulation baths containing (A) 100% (v/v) and (B)  
309 75% (v/v) ethanol and different AP concentrations: (i) 0.1%, and (ii) 0.5% (v/v) of the  
310 coagulation bath.



311  
 312 **Fig. 10.** DSC curves of starch fibers from coagulation baths containing (A) 100% (v/v) and (B)  
 313 75% (v/v) ethanol and different AP concentrations: (i) 0.1%, and (ii) 0.5% (w/v) of the  
 314 coagulation bath.

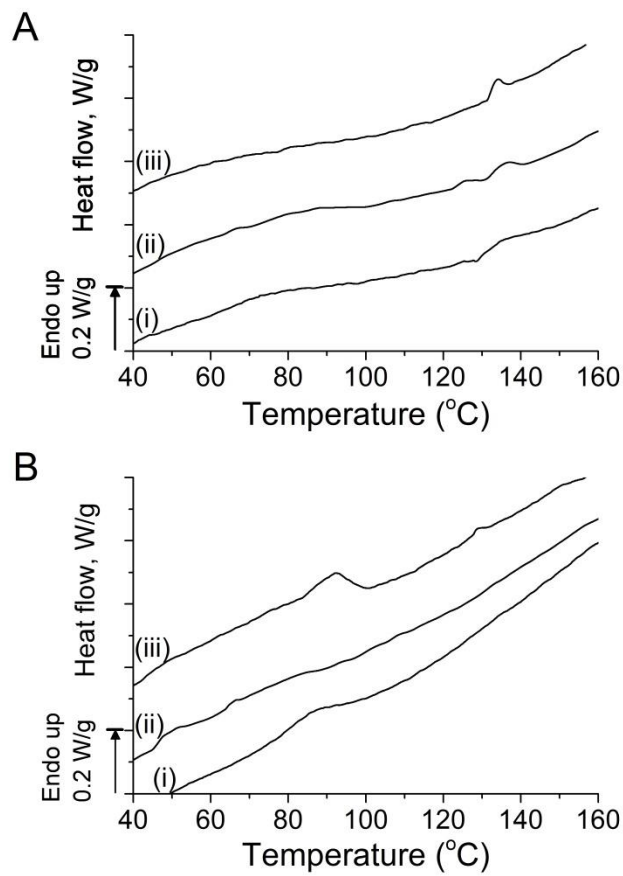
315 The presence of CTAB in the starch fibers from 75% ethanol with 2% CTAB could be  
 316 detected in FTIR spectra, with characteristic bands at 720, 960 (shoulder), 1461, 1479, 2850, and  
 317 2915  $\text{cm}^{-1}$  (Fig. 11). The 2850 and 2915  $\text{cm}^{-1}$  bands, which have been assigned to the  $\text{CH}_2$   
 318 stretching vibrations of alkyl chain were more apparently seen than other bands that might have  
 319 been shielded by starch bands (Sui et al., 2006). This fiber sample showed a single narrow  
 320 endotherm with a peak temperature at 92 °C (Fig. 12). The starch-CTAB inclusion complexes  
 321 demonstrated the same thermal stability as the starch-AP inclusion complexes. It was expected  
 322 that the two types of inclusion complex have the same length, because both CTAB and AP have  
 323 C16 hydrocarbon chain. By the bath mixing method, inclusion complex formation in fibers

324 requires a higher amount of CTAB, i.e. 2%, than the amount of AP, i.e. 0.5%, in the 75% ethanol  
325 coagulation bath.



326

327 **Fig. 11.** FTIR spectra of (i) CTAB powder sample and starch fibers from coagulation baths  
328 containing 2% (w/v) CTAB in (ii) 75% (v/v) and (iii) 100% (v/v) ethanol.



329

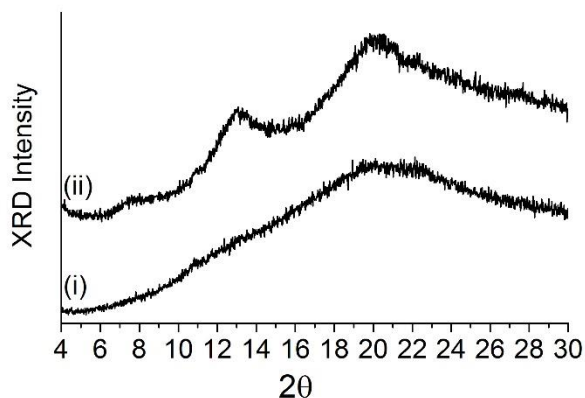
330 **Fig. 12.** DSC curves of starch fibers from coagulation baths containing (A) 100% (v/v) and (B)  
331 75% (v/v) ethanol and different CTAB concentrations: (i) 0.1%, (ii) 1%, and (iii) 2% (w/v) of the  
332 coagulation bath.

### 333 **3.3. The effect of native lipids**

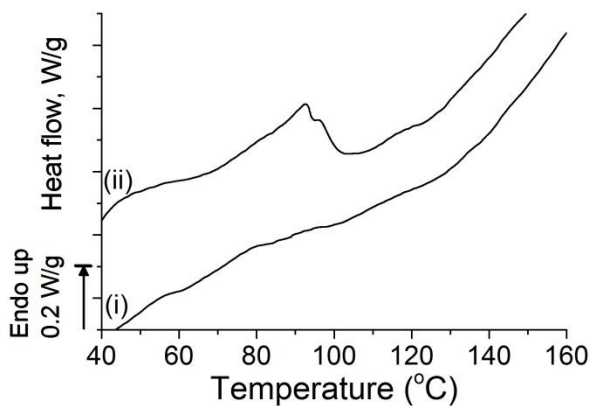
334 High-amylose starch contains approximately 1% (w/w, dry starch) of native lipids, which  
335 are primarily composed of palmitic, stearic, and linoleic acid, in the form of free fatty acids and  
336 lysophospholipids (Morrison, 1988). These fatty acids have alkyl chains long enough to form  
337 stable inclusion complexes with amylose helices. Native lipids have been found to enhance the  
338 complexation between starch and certain guest compounds (Tapanapunnitikul, Chaiseri,  
339 Peterson, & Thompson, 2007). The native lipids may also play an important role in the inclusion  
340 complex formation in the electrospun starch fibers. Therefore, lipid-free starch was used for  
341 electrospinning to determine if the presence of native lipids is a necessity for inclusion complex  
342 formation in the starch fibers.

343 The electrospun lipid-free starch fibers recovered from 75% ethanol bath showed V-type  
344 diffraction patterns (Fig. 13). Without guest molecules, starch would precipitate out of solution  
345 by simple retrogradation in conventional inclusion complex preparation methods, which would  
346 result in a B-type X-ray diffraction pattern. Fast collapse of starch from ethanol resulted in single  
347 helices and V-type crystallinity without the presence of guest molecules. The lipid-free starch  
348 fibers showed a very low and broad endotherm that is similar to regular starch fibers recovered  
349 from 100% ethanol (Fig. 14). Without guest lipids, this suggested that the low and broad  
350 endotherm could be associated with retrogradation of the amylopectin fraction (Kohyama &  
351 Nishinari, 1991). Starch-AP fibers were prepared by electrospinning lipid-free starch using the  
352 dope mixing method. An endothermic peak at around 93 °C was observed, which is consistent

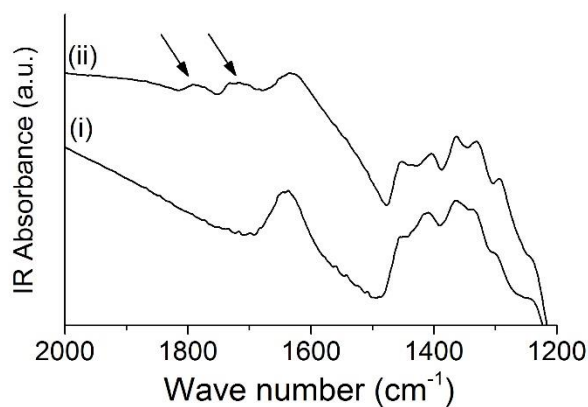
353 with the behavior of starch containing native lipids. The presence of AP in the starch fibers was  
354 also evidenced by the carbonyl bands ( $1730$  and  $1778\text{ cm}^{-1}$ ) on IR spectrum (Fig. 15). In  
355 conclusion, there were no differences in inclusion complex formation between raw starch and  
356 lipid-free starch.



357  
358 **Fig. 13.** X-ray diffraction patterns of lipid-free starch fibers recovered from coagulation bath  
359 containing (i) 100% and (ii) 75% (v/v) ethanol.



360  
361 **Fig. 14.** DSC curves of (i) lipid-free starch fibers and (ii) starch-AP (5%, w/w) fibers from lipid-  
362 free starch spun into 75% (v/v) ethanol.



363  
 364 **Fig. 15.** FTIR spectra of lipid-free starch-AP (5%, w/w) fibers recovered from (i) 100% and (ii)  
 365 75% (v/v) ethanol.

#### 366 4. Conclusions

367 Selected guest compounds, i.e. palmitic acid, ascorbyl palmitate, and cetyl-  
 368 trimethylammonium bromide, formed inclusion complexes with starch in electrospun starch  
 369 fibers. Two different methods were employed: dope mixing method and bath mixing method.  
 370 Using 100% ethanol as the coagulation bath was not as efficient as 75% ethanol in inducing  
 371 inclusion complex formation, probably due to the fast collapse of starch. Native lipids were not  
 372 required to induce the inclusion complex formation during electrospinning. Formation of  
 373 inclusion complexes in fibers was less efficient than previously used DMSO method, because  
 374 time was limited for the guest compounds to enter the helices and the helices to arrange  
 375 themselves in a regular order. A minimum amount of guest was required that depended on  
 376 method and guest chemistry. The electrospun starch fibers are potentially useful for delivery of  
 377 bioactive compounds. It would be worthwhile to try to encapsulate more types of nutrients,  
 378 drugs, and bioactive molecules, intended for biomedical applications, for instance, wound  
 379 dressings based on starch fibers.

380 **Supplementary material**

381 FTIR spectra of palmitic acid, ascorbyl palmitate, and Hylon VII starch (Fig. A.); DSC  
382 scanning curves of Hylon VII starch-PA and starch-AP inclusion complexes made by DMSO  
383 method (Fig. B.).

384 **Acknowledgement**

385 This work is funded by the USDA National Institute for Food and Agriculture, National  
386 Competitive Grants Program, National Research Initiative Program 71.1 FY 2007 as grant #  
387 2007-35503-18392.

388

389 **References**

- 390 Bhosale, R. G., & Ziegler, G. R. (2010). Preparation of spherulites from amylose–palmitic acid  
391 complexes. *Carbohydrate Polymers*, 80(1), 53–64.
- 392 Biais, B., Le Bail, P., Robert, P., Pontoire, B., & Buléon, A. (2006). Structural and stoichiometric  
393 studies of complexes between aroma compounds and amylose. Polymorphic transitions and  
394 quantification in amorphous and crystalline areas. *Carbohydrate Polymers*, 66(3), 306–315.
- 395 Biliaderis, C. G., & Galloway, G. (1989). Crystallization behavior of amylose-V complexes:  
396 Structure-property relationships. *Carbohydrate Research*, 189(0), 31–48.
- 397 Biliaderis, C. G., Page, C. M., Slade, L., & Sirett, R. R. (1985). Thermal behavior of amylose-  
398 lipid complexes. *Carbohydrate Polymers*, 5(5), 367–389.
- 399 Bluhm, T. L., & Zugenmaier, P. (1981). Detailed structure of the Vh-amylose-iodine complex: a  
400 linear polyiodine chain. *Carbohydrate Research*, 89(1), 1–10.
- 401 Cohen, R., Orlova, Y., Kovalev, M., Ungar, Y., & Shimoni, E. (2008). Structural and functional  
402 properties of amylose complexes with genistein. *Journal of Agricultural and Food*  
403 *Chemistry*, 56(11), 4212–4218.
- 404 Conde-Petit, B., Escher, F., & Nuessli, J. (2006). Structural features of starch-flavor  
405 complexation in food model systems. *Trends in Food Science & Technology*, 17(5), 227–  
406 235.
- 407 Eliasson, A. C. (1988). On the thermal transitions of the amylose-cetyltrimethylammonium  
408 bromide complex. *Carbohydrate Research*, 172(1), 83–95.
- 409 Helbert, W., & Chanzy, H. (1994). Single crystals of V amylose complexed with n-butanol or n-  
410 pentanol: structural features and properties. *International journal of biological*  
411 *macromolecules*, 16(4), 207–213.
- 412 Klucinec, J. D., & Thompson, D. B. (1998). Fractionation of high-amylose maize starches by  
413 differential alcohol precipitation and chromatography of the fractions. *Cereal chemistry*,  
414 75(6), 887–896.
- 415 Kohyama, K., & Nishinari, K. (1991). Effect of soluble sugars on gelatinization and  
416 retrogradation of sweet potato starch. *Journal of Agricultural and Food Chemistry*, 39(8),  
417 1406–1410.
- 418 Kong, L., & Ziegler, G. R. (2012a). Patents on fiber spinning from starches. *Recent Patents on*  
419 *Food, Nutrition & Agriculture*, 4(3), 210–219.
- 420 Kong, L., & Ziegler, G. R. (2012b). Role of molecular entanglements in starch fiber formation  
421 by electrospinning. *Biomacromolecules*, 13(8), 2247–53.

- 422 Kong, L., & Ziegler, G. R. (2013). Quantitative relationship between electrospinning parameters  
423 and starch fiber diameter. *Carbohydrate Polymers*, 92(2), 1416–1422.
- 424 Kong, L., & Ziegler, G. R. (2014). Fabrication of pure starch fibers by electrospinning. *Food*  
425 *Hydrocolloids*, 36(0), 20–25.
- 426 Lalush, I., Bar, H., Zakaria, I., Eichler, S., & Shimoni, E. (2004). Utilization of amylose–lipid  
427 complexes as molecular nanocapsules for conjugated linoleic acid. *Biomacromolecules*,  
428 6(1), 121–130.
- 429 Lay Ma, U. V., Floros, J. D., & Ziegler, G. R. (2011). Formation of inclusion complexes of  
430 starch with fatty acid esters of bioactive compounds. *Carbohydrate Polymers*, 83(4), 1869–  
431 1878.
- 432 Lesmes, U., Barchechath, J., & Shimoni, E. (2008). Continuous dual feed homogenization for the  
433 production of starch inclusion complexes for controlled release of nutrients. *Innovative*  
434 *Food Science and Emerging Technologies*, 9(4), 507–515.
- 435 Lesmes, U., Cohen, S. H., Shener, Y., & Shimoni, E. (2009). Effects of long chain fatty acid  
436 unsaturation on the structure and controlled release properties of amylose complexes. *Food*  
437 *Hydrocolloids*, 23(3), 667–675.
- 438 Morrison, W. R. (1988). Lipids in cereal starches: A review. *Journal of Cereal Science*, 8(1), 1–  
439 15.
- 440 Oguchi, T., Yamasato, H., Limmatvapirat, S., Yonemochi, E., & Yamamoto, K. (1998).  
441 Structural change and complexation of strictly linear amylose induced by sealed-heating  
442 with salicylic acid. *Journal of the Chemical Society, Faraday Transactions*, 94(7), 923–927.
- 443 Pozo-Bayon, M. A., Biais, B., Rampon, V., Cayot, N., & Le Bail, P. (2008). Influence of  
444 complexation between amylose and a flavored model sponge cake on the degree of aroma  
445 compound release. *Journal of Agricultural and Food Chemistry*, 56(15), 6640–6647.
- 446 Putseys, J. A., Lamberts, L., & Delcour, J. A. (2010). Amylose-inclusion complexes: Formation,  
447 identity and physico-chemical properties. *Journal of Cereal Science*, 51(3), 238–247.
- 448 Raphaelides, S., & Karkalas, J. (1988). Thermal dissociation of amylose-fatty acid complexes.  
449 *Carbohydrate Research*, 172(1), 65–82.
- 450 Rondeau-Mouro, C., Bail, P. Le, & Buléon, A. (2004). Structural investigation of amylose  
451 complexes with small ligands: inter- or intra-helical associations? *International Journal of*  
452 *Biological Macromolecules*, 34(5), 251–257.
- 453 Shimoni, E. (2008). Starch as an encapsulation material to control digestion rate in the delivery  
454 of active food components. In N. Garti (Ed.), *Delivery and controlled release of bioactives*  
455 *in foods and nutraceuticals* (pp. 279–293). Cambridge, UK: Woodhead Publishing Ltd.

- 456 Sui, Z. M., Chen, X., Wang, L. Y., Xu, L. M., Zhuang, W. C., Chai, Y. C., & Yang, C. J. (2006).  
457 Capping effect of CTAB on positively charged Ag nanoparticles. *Physica E: Low-*  
458 *dimensional Systems and Nanostructures*, 33(2), 308–314.
- 459 Tapanapunnitikul, O., Chaiseri, S., Peterson, D. G., & Thompson, D. B. (2007). Water solubility  
460 of flavor compounds influences formation of flavor inclusion complexes from dispersed  
461 high-amylose maize starch. *Journal of Agricultural and Food Chemistry*, 56(1), 220–226.
- 462 Tozuka, Y., Takeshita, A., Nagae, A., Wongmekiat, A., Moribe, K., Oguchi, T., & Yamamoto, K.  
463 (2006). Specific Inclusion Mode of Guest Compounds in the Amylose Complex Analyzed  
464 by Solid State NMR Spectroscopy. *Chemical and Pharmaceutical Bulletin*, 54(8), 1097–  
465 1101.
- 466 Tufvesson, F., Wahlgren, M., & Eliasson, A. (2003). Formation of amylose-lipid complexes and  
467 effects of temperature treatment. Part 2. fatty acids. *Starch-Stärke*, 55(3-4), 138–149.
- 468 Uchino, T., Tozuka, Y., Oguchi, T., & Yamamoto, K. (2002). Inclusion compound formation of  
469 amylose by sealed-heating with salicylic acid analogues. *Journal of Inclusion Phenomena*  
470 *and Macrocyclic Chemistry*, 43(1), 31–36.
- 471 Whittam, M. A., Orford, P. D., Ring, S. G., Clark, S. A., Parker, M. L., Cairns, P., & Miles, M. J.  
472 (1989). Aqueous dissolution of crystalline and amorphous amylose-alcohol complexes.  
473 *International Journal of Biological Macromolecules*, 11(6), 339–344.
- 474 Winter, W. T., & Sarko, A. (1974). Crystal and molecular structure of V-anhydrous amylose.  
475 *Biopolymers*, 13(7), 1447–1460.
- 476 Yang, L., Zhang, B., Yi, J., Liang, J., Liu, Y., & Zhang, L. (2013). Preparation, characterization,  
477 and properties of amylose-ibuprofen inclusion complexes. *Starch-Stärke*, 65(7-8), 593–602.
- 478 Yang, Y., Gu, Z., & Zhang, G. (2009). Delivery of bioactive conjugated linoleic acid with self-  
479 assembled amylose–CLA complex. *Journal of Agricultural and Food Chemistry*, 57(15),  
480 7125–7130.
- 481 Zahedi, P., Rezaeian, I., Ranaei-Siadat, S. O., Jafari, S. H., & Supaphol, P. (2010). A review on  
482 wound dressings with an emphasis on electrospun nanofibrous polymeric bandages.  
483 *Polymers for Advanced Technologies*, 21(2), 77–95.

484

485

486 **Figure captions**

487 **Fig. 1.** Schematic drawing of the electro-wet-spinning setup and two routes of starch-guest  
488 inclusion complex formation during electrospinning. Orange curves show the conformation of  
489 starch molecules and blue ovals stand for guest molecules. Grey arrows show the diffusion of  
490 guest molecules either into or out of the precipitated fibers.

491 **Fig. 2.** Scanning electron micrograph of starch-palmitic acid fibers from coagulation bath  
492 containing 75% (v/v) ethanol.

493 **Fig. 3.** X-ray diffraction patterns of (A) starch without guest, (B) starch-palmitic acid, and (C)  
494 starch-ascorbyl palmitate fibers from coagulation baths containing (i) 100% and (ii) 75% (v/v)  
495 ethanol, respectively.

496 **Fig. 4.** FTIR spectra of starch-palmitic acid (PA) fibers from coagulation baths containing (A)  
497 100% (v/v) and (B) 75% (v/v) ethanol, with different PA levels in spinning dope: (i) 1%, (ii)  
498 2.5%, and (iii) 5% (w/w) of starch. Arrows indicate the band for PA.

499 **Fig. 5.** FTIR spectra of starch-ascorbyl palmitate (AP) fibers from coagulation baths containing  
500 (A) 100% (v/v) and (B) 75% (v/v) ethanol, with different AP levels in spinning dope: (i) 1%, and  
501 (ii) 5% (w/w) of starch. Arrows indicate the band for AP.

502 **Fig. 6.** DSC curves of starch-palmitic acid (PA) fibers from coagulation baths containing (A)  
503 100% (v/v) and (B) 75% (v/v) ethanol, with different PA levels in spinning dope: (i) 1%, (ii)  
504 2.5%, and (iii) 5% (w/w) of starch.

505 **Fig. 7.** DSC curves of starch-ascorbyl palmitate (AP) fibers from coagulation baths containing  
506 (A) 100% (v/v) and (B) 75% (v/v) ethanol, with different AP levels in spinning dope: (i) 1%, and  
507 (ii) 5% (w/w) of starch.

508 **Fig. 8.** X-ray diffraction patterns of starch fibers from coagulation baths containing (A) 0.5%  
509 (w/v) AP and (B) 2% (w/v) CTAB in (i) 100% and (ii) 75% (v/v) ethanol, respectively.

510 **Fig. 9.** FTIR spectra of starch fibers from coagulation baths containing (A) 100% (v/v) and (B)  
511 75% (v/v) ethanol and different AP concentrations: (i) 0.1%, and (ii) 0.5% (v/v) of the  
512 coagulation bath.

513 **Fig. 10.** DSC curves of starch fibers from coagulation baths containing (A) 100% (v/v) and (B)  
514 75% (v/v) ethanol and different AP concentrations: (i) 0.1%, and (ii) 0.5% (w/v) of the  
515 coagulation bath.

516 **Fig. 11.** FTIR spectra of (i) CTAB powder sample and starch fibers from coagulation baths  
517 containing 2% (w/v) CTAB in (ii) 75% (v/v) and (iii) 100% (v/v) ethanol.

518 **Fig. 12.** DSC curves of starch fibers from coagulation baths containing (A) 100% (v/v) and (B)  
519 75% (v/v) ethanol and different CTAB concentrations: (i) 0.1%, (ii) 1%, and (iii) 2% (w/v) of the  
520 coagulation bath.

521 **Fig. 13.** X-ray diffraction patterns of lipid-free starch fibers recovered from coagulation bath  
522 containing (i) 100% and (ii) 75% (v/v) ethanol.

523 **Fig. 14.** DSC curves of (i) lipid-free starch fibers and (ii) starch-AP (5%, w/w) fibers from lipid-  
524 free starch spun into 75% (v/v) ethanol.

525 **Fig. 15.** FTIR spectra of lipid-free starch-AP (5%, w/w) fibers recovered from (i) 100% and (ii)  
526 75% (v/v) ethanol.